

Cool Concrete Incorporating Carbonated Periwinkle Shell: A Sustainable Solution for Mitigating Urban Heat Island Effects

Guido Goracci,* Ebtisam Saeed, Mary B. Ogundiran, Amaia Iturrospe, Arantxa Arbe, Cyril Aymonier, and Jorge S. Dolado

Cite This: *ACS Sustainable Chem. Eng.* 2024, 12, 1911–1917

Read Online

ACCESS |

Metrics & More

Article Recommendations

ABSTRACT: The urban heat island effect has become a critical issue in urban areas, intensifying heat-related problems and increasing energy consumption. A sustainable cement formulation that combines ordinary Portland cement (OPC) with a carbonated aggregate derived from Periwinkle shell powder for the development of an efficient cool material is presented. Through a carbonation process, the aggregate undergoes a transformation, capturing carbon dioxide (CO₂) and converting it into calcite. The resulting cement mixture exhibits high solar reflective properties, making it a potential candidate for cool pavement and roof applications. In this study, the raw materials, including the Periwinkle shell powder, were characterized, and the carbonation process was evaluated to quantify the CO₂ capture efficiency.

Additionally, a real test of the efficiency of this new cement on a roof demonstrated that the material achieved a significant cooling effect, being 6 °C cooler than that with standard OPC at the peak of solar radiation.

KEYWORDS: urban heat island, carbon capture, cool material, carbonated aggregates, recycled aggregates, cementitious material



INTRODUCTION

Urban heat Island (UHI) is a significant problem facing cities today, wherein urban areas tend to experience higher temperatures compared to those of surrounding rural areas. The elevated temperature in cities is primarily attributed to the high density of paved and roofed surfaces, such as roads, sidewalks, and building roofs, which absorb and retain heat. This phenomenon leads to increased energy consumption for cooling, reduced human comfort, and adverse impacts on the local environment and biodiversity. In recent years, various strategies have been proposed to mitigate the effects of UHI,^{1,2} including the use of green roofs,^{3–5} blue infrastructures,⁶ and cool pavements and roofs.^{7–9} Regarding this last strategy, studies are mainly centered on the development of reflective coatings^{10–13} and thermochromic materials.^{14–16} However, these solutions have several limitations that hinder their widespread adoption. For instance, many reflective surfaces and cool roof membranes have a relatively short lifespan and require frequent maintenance, while the installation and maintenance costs of green roofs can be substantial. In this context, the utilization of sustainable construction materials with high solar reflectivity and emissivity in the atmospheric window can enhance the overall energy performance of buildings while reducing maintenance needs. Moreover, such a cost-effective approach not only contributes to the reduction

of carbon emission associated with energy consumption for cooling purposes but also addresses the carbon footprint during their production. One promising solution for sustainable construction is the use of carbonated concrete, which involves converting carbon dioxide (CO₂) into a solid mineral that can be permanently stored, preventing its release into the atmosphere. This process has the potential to play a crucial role in reducing greenhouse gas emissions and mitigating global warming.^{17,18} Carbon capture processes have proven to be effective for both fresh and hardened Portland cement, resulting in significant improvements in the mechanical properties of the resulting cementitious materials. Additionally, the utilization of recycled concrete or artificial aggregates offers an opportunity to store CO₂ and mitigate the carbon dioxide emissions associated with cement production. However, it is important to note that the current literature primarily focuses on the mechanical properties of carbonated concretes,^{19–28} without paying attention to secondary func-

Received: September 11, 2023

Revised: December 20, 2023

Accepted: December 21, 2023

Published: January 19, 2024

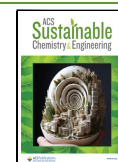


Table 1. Oxide Composition of Materials (wt %)

material	SiO ₂	Al ₂ O ₃	Fe ₂ O ₃	MnO	MgO	CaO	Na ₂ O	K ₂ O	Ti ₂ O	P ₂ O ₅	SO ₃
PS	1.28	0.52	0.42	0.05	0.70	59.5	0.48	0.15	0.02	0.10	0.17
OPC clinker	19.0	4.73	2.79	0.02	1.05	62.7	0.01	0.94	0.24	0.17	2.70



Figure 1. Overview of the experimental setup of carbonation of Periwinkle shell ash.

tional properties such as reflectivity. By incorporating highly solar reflective carbonated aggregates into the concrete matrix, sustainable construction materials that not only sequester CO₂ but also possess desirable reflective properties can be developed. To address this research gap, the reflective properties of an innovative cool cementitious composite that incorporates a novel carbonated aggregate derived from recycled Periwinkle shells was studied. Periwinkles are a type of sea snail commonly found worldwide, and their shells primarily consist of portlandite and calcite. Through a carefully controlled carbon capture process, we were able to transform the Periwinkle shell ash into carbonated aggregates. In fact, the strong reactivity with carbon dioxide of portlandite, and its subsequent conversion to calcite ($\text{Ca}(\text{OH})_2 + \text{CO}_2 \rightarrow \text{CaCO}_3 + \text{H}_2\text{O}$), is well reported in literature.^{29,30} The resulting carbonated Periwinkle shell (CPS) ash was mixed with ordinary Portland cement (OPC) at a ratio of 70 wt % CPS ash,³¹ leading to the production of reflective concrete. This proportion was deliberately chosen to align with the typical aggregate content, encompassing both coarse and fine components commonly employed in standard concrete mixes. Remarkably, this cool concrete captured approximately 18 wt % of its weight in carbon dioxide and achieved a competitive solar reflectance index (SRI) of 73. To evaluate the performance of OPCCPS as a cool material, a comparative experiment was conducted on a sunny day. The OPCCPS samples were tested alongside standard cement paste samples on a rooftop under a solar power radiation ranging from 580 to 980 W/m² for a duration of 7 h. The results demonstrated the excellent performance of the concrete with carbonated aggregate as it effectively reduced the maximum surface temperature by 6 °C. This reduction is comparable to that by the state-of-the-art reflective pavements,^{32,33} highlighting the potential of carbonated aggregates as an effective solution for mitigating urban heat island effects. Furthermore, it is important to highlight the simplicity and scalability of our carbon capture process. The method employed in our study presents an exceptionally straightforward approach to convert carbon dioxide to a stable mineral form. This streamlined process holds tremendous promise for widespread implementation in sustainable construction practices, offering an accessible solution to the critical issue of carbon emissions.

EXPERIMENTAL SECTION

Materials and Sample Preparation. The raw materials used in this study were OPC CEM-1 52.5R (Rezola) and Periwinkle shell (PS) ash. The oxide compositions of these materials are presented in Table 1. To prepare CPS, a mixture of 5 g of PS ash and 87.5 mL of distilled water was placed in a sealed plastic tube (Figure 1). The CO₂ gas with a pressure of 0.4 bar was then bubbled into the mixture while stirring at a speed of 1700 rpm for 15 min at room temperature. Subsequently, the sample was immersed in a water-rich CO₂ environment overnight. The resulting carbonated Periwinkle powder was obtained by centrifugation for 10 min followed by drying at 80 °C overnight. For the production of the cement paste samples, the cement was first mixed with carbonated Periwinkle (CPS) using a cement-to-ash ratio of 0.3. Water was then added at a water-to-cement (w/c) ratio of 1, along with a superplasticizer at a concentration of 6 wt % relative to that of the OPC. The mixture was stirred for 90 s, allowed to rest for 60 s, and then stirred again for an additional 90 s. The resulting mixture was poured into a silicon mold and left to cure in a desiccator with a relative humidity of 100% for 24 h.

Methods. To identify the distinct phases through the comparison of the characteristic functional groups, PS and CPS were characterized using Fourier transform infrared (FTIR), a Jasco 6300, with a spectral range of 4000–500 cm⁻¹. The experiments were carried out under ambient conditions. The vibrational absorption spectra of the samples were captured using an attenuated total reflectance (ATR) configuration, employing a single-reflection diamond ATR from Specac, equipped with a N₂ purge. The carbonation efficiency of the PS and OPCCPS was evaluated by thermogravimetric analysis (TGA) using a TGA-500 instrument (TA Instruments). Approximately 10 mg of CPS powder was heated from room temperature to 900 °C at a rate of 10 °C/min under a flow of nitrogen gas. Diffraction experiments were conducted with a Bruker X-ray diffractometer (D8 ADVANCE, US) using Cu K α radiation ($\lambda = 1.5418 \text{ \AA}$). A scattering angle (2θ) range from 5 to 90° was covered with a scan rate of 0.05°. The average measuring time was 50 s/point. The SRI of the cement paste was determined by measuring the solar reflectivity from ultraviolet (UV) to mid-infrared (MIR) using a portable spectrophotometer (410-SOLAR) and an integrated sphere mounted on FTIR (PIKE). Three measurements were performed on each sample, and the average value was reported. Furthermore, to evaluate the performance of concrete with carbonated aggregates (OPCCPS), a comparative analysis was conducted using plain OPC cement paste as a reference. Solar radiation exposure tests were carried out on a sunny day on the roof, and the surface temperatures of both OPCCPS and plain OPC cement paste specimens were monitored. The measurements were conducted between 9:30 am and 4:30 pm local time to capture the peak solar intensity and assess the materials' response during the most critical hours of the day. Solar power radiation was

measured using a pyranometer (APOGEE SP510), capable of measuring in the spectral range of 385–2105 nm. The surface temperature of the specimens was monitored using an infrared thermometer (BOSCH GTC 600C). Additionally, wind speed was measured using a sonic anemometer (METER ATMOS 22) to account for temperature changes induced by wind. During the solar radiation exposure tests, temperature readings were taken every 30 min to monitor the surface temperature of the samples. Solar power radiation and wind speed measurements were recorded at 5 min intervals to capture the variations in solar intensity and wind conditions. This frequent data collection allowed for a comprehensive assessment of the thermal behavior of both OPCCPS and plain OPC cement paste under varying environmental conditions. The prototype, as depicted in Figure 2, facilitated simultaneous monitoring of



Figure 2. Prototype for assessing cooling performance under solar radiation.

temperature, solar radiation, and wind speed, providing valuable insights into the performance of OPCCPS relative to the plain OPC cement paste reference during the test period.

RESULTS AND DISCUSSION

Material Characterization. The FTIR results of the PS are presented in Figure 3a. The analysis reveals three

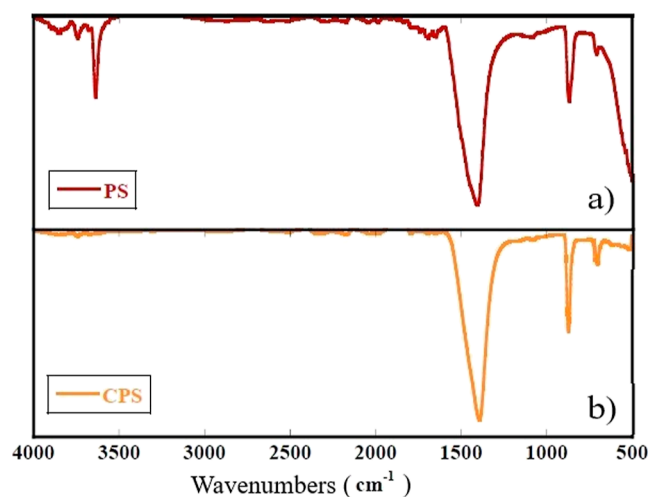


Figure 3. FTIR analysis results of PS (a) and CPS (b).

prominent peaks in the wavelength range investigated. The peak at 3645 cm^{-1} is associated with the stretching of OH bonds in portlandite, while peaks at 1420 and 875 cm^{-1} are related to vibrations of carbonated groups in calcite, respectively, asymmetric stretching, out of plane bending and split in-plane bend the presence of calcite.^{27,34} Finally, the

decrease at low wavenumbers is a characteristic feature of the portlandite spectrum. Hence, FTIR measurements revealed that PS is mainly composed of portlandite and calcite. These findings are further supported by the X-ray diffraction (XRD) pattern shown in Figure 4a, where these phases are identified

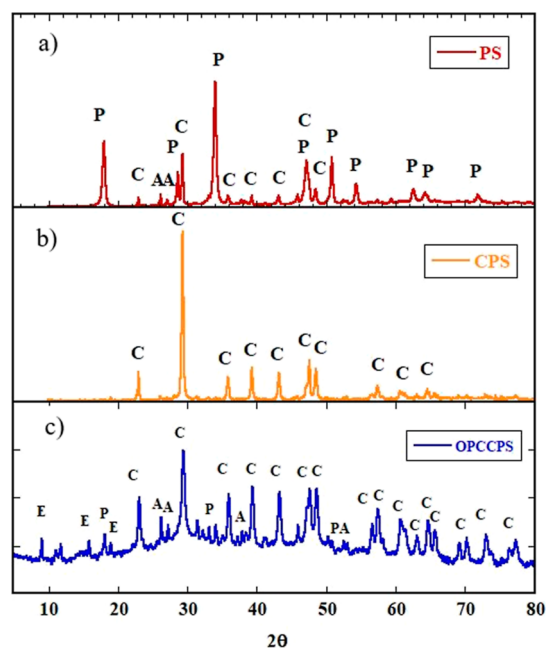


Figure 4. XRD patterns of PS (a), CPS (b), and OPCCPS (c). P: Portlandite, C: Calcite, E: Ettringite, and A: Aragonite.

as the primary constituents. The carbon capture process applied to the PS resulted in the formation of a CPS, predominantly composed of calcite. This is evidenced by the FTIR spectrum and the XRD patterns where contributions from portlandite disappeared (see Figures 3b and 4b). Finally, the TGA curve of CPS (Figure 5a) exhibits a significant decay between 600 and 700 °C ,³⁵ indicating the decarbonation of the calcite formed during the carbonation reaction of the PS. Regarding the concrete with carbonated aggregates (OPCCPS), the XRD pattern (Figure 4c) reveals the presence of an amorphous phase halo typical of cement gel matrix, along with characteristic peaks associated with the hydration products of OPC, such as ettringite and portlandite.³⁶ Additionally, distinct and intense peaks corresponding to calcite are detected, indicating the presence of the carbonated aggregate (CPS). The TGA curve of OPCCPS, depicted in Figure 5b, exhibits weight loss attributed to the evaporation of bulk water at temperatures below 150 °C . The dehydroxylation of portlandite is observed at approximately 400 °C .³⁷ Since the conversion of portlandite in PS to calcite is complete after the carbon capture process, the weight loss observed in this region is solely attributed to the OPC hydration process, where portlandite is one of the components. Furthermore, a significant weight decrease associated with CO_2 loss is evident, indicating an uptake of 18 wt % of carbon dioxide. The observed decrease in intensity, compared with that in pure CPS, is consistent with the percentage of CPS present in the OPCCPS sample.

Reflective Property Analysis. The measured reflectance of the CPS is presented in Figure 6a. In the sun wavelength–frequency range (yellow area), a pronounced peak in

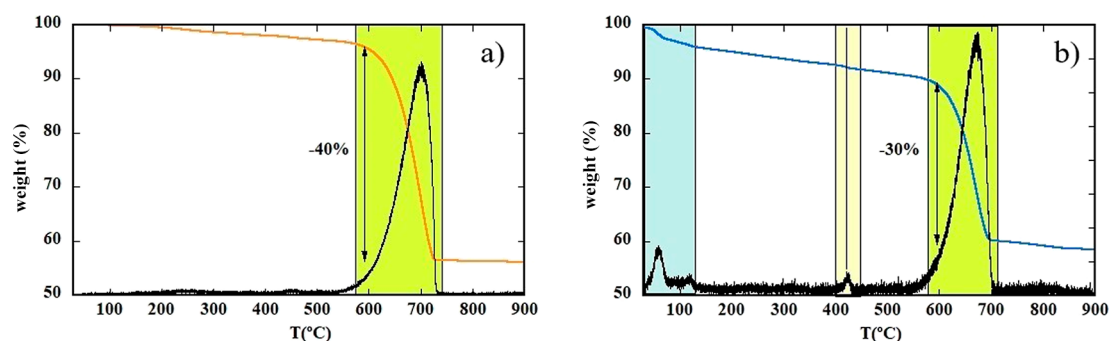


Figure 5. TGA curves and derivative curves of the CPS (a) and OPCCPS (b). The blue area represents the weight loss associated with the evaporation of bulk water, the yellow area corresponds to the dehydroxylation of portlandite, and the green area indicates the decomposition of calcite.

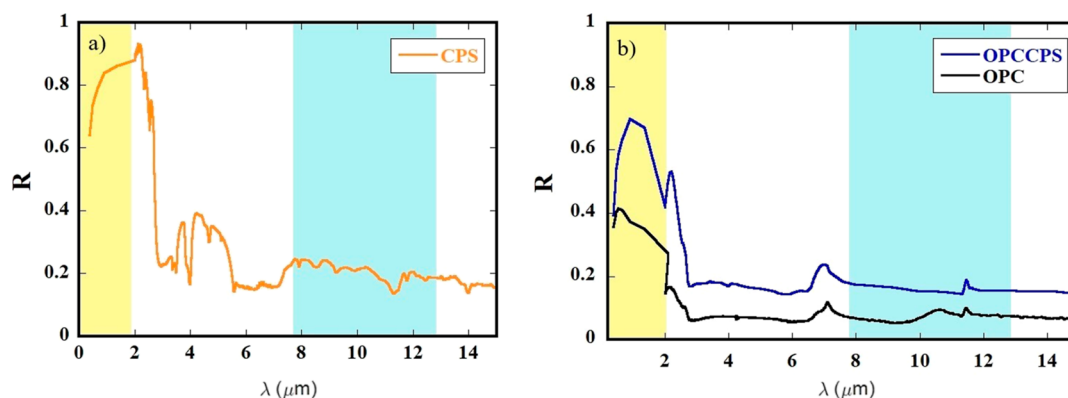


Figure 6. Reflectance properties of CPS (a) and comparison of reflectance between OPCCPS and OPC (b). The yellow area represents the solar window, which encompasses the wavelength range of solar radiation, while the light blue area corresponds to the atmosphere window.

reflectance R was observed. To determine the solar absorption (α) of the cementitious composite, the data were normalized to the solar spectra (ASTM G173 Global Solar spectrum), resulting in a calculated value of $\alpha = 0.11$. This remarkably low value not only outperforms those of commonly used cool paving materials³⁸ (0.23–0.4) but also falls within the recommended range of 0.05–0.125 for achieving subambient cooling.³⁹ This result highlights the potential of CPS as an additive for the development of effective cooling materials. To provide context in comparison with other materials used as cool materials, CPS exhibits values lower than TiO_2 ($\alpha > 0.17$),³⁹ a metal oxide commonly employed for white coating with high reflectivity. Additionally, the solar absorption value of CPS is comparable to that of Portlandite ($\alpha = 0.07$),⁴⁰ another mineral known for its low solar absorption. In the frequency range within the atmospheric window (light blue area), an almost flat R can be observed, with a small dip at around 11 μm . Regarding the concrete with carbonated aggregates OPCCPS, the reflectance R is shown in Figure 6b with standard OPC used as the reference. The lower values of R observed in the solar windows of the OPC can primarily be attributed to the presence of ferrite in the OPC clinker. Given that reflectivity in solar windows is directly correlated with the whiteness of the cementitious material, the inclusion of ferrite in the OPC contributes to a darker color resulting in reduced reflectance. Compared to that in OPC, a remarkable enhancement in reflectance (+62%) was evident in the sample utilizing carbonated aggregates, exhibiting a solar absorption coefficient α of 0.38. This notable improvement can be attributed to the substantial presence of calcite resulting from

the carbonation of the PS. Indeed, calcite functions as an effective whitening agent, contributing significantly to the heightened reflectance. In the atmospheric window, the OPCCPS exhibits higher reflectance values than the reference due to the high content of calcite. This aligns with previous observations of the inferior performance of calcite in this range, as reported by Liu et al.⁴¹ One common method to quantify the cooling efficiency is the estimation of their SRI, which is calculated using solar reflectance and thermal emissivity values adjusted with wind coefficients. According to the active standard ASTM E1980, SRI is defined by the equation

$$\text{SRI} = 123.97 - 141.35\chi + 9.665\chi^2 \quad (1)$$

with

$$\chi = (\alpha - 0.029\epsilon) \times (8.797 + h_c) / (9.52\epsilon + h_c) \quad (2)$$

where α is the solar absorbance ($1 - R$), ϵ the emissivity, and h_c the convective heat transfer coefficient. In order to calculate the SRI, the emissivity ϵ was calculated as $1 - \langle R \rangle$, where $\langle R \rangle$ is the average of R in the atmospheric window. Assuming a modest value of $h_c = 10 \text{ W/m}^2\text{K}$, an SRI = 73 was obtained for OPCCPS. Additionally, to further assess the cooling performance of OPCCPS, a comprehensive test was conducted on the rooftop of the Centro de Física de Materiales in San Sebastian, Spain, during a sunny day from 9:30 to 16:30. The solar radiation power during the test ranged from 580 to 980 W/m^2 . The results of this evaluation are depicted in Figure 7. It is evident from the surface temperature measurements (Figure 7d) that the carbonated concrete consistently exhibits lower temperatures compared to that of the OPC paste, with a

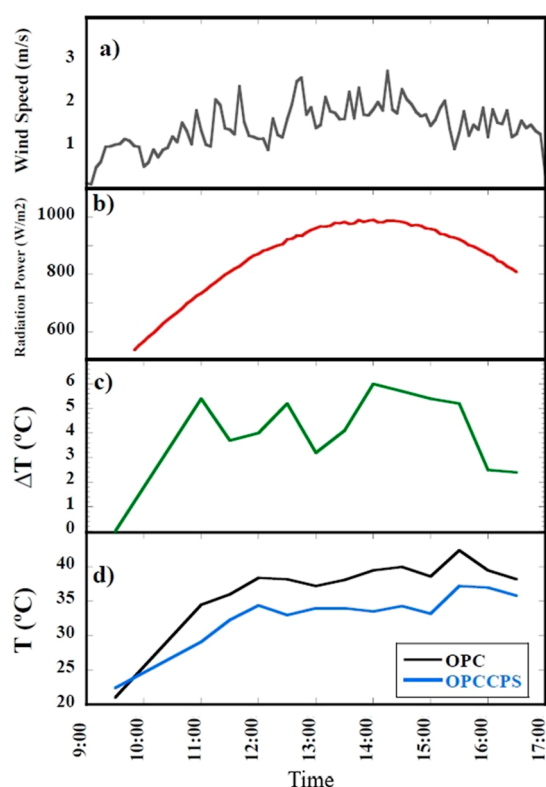


Figure 7. Results of the cool performance test of the OPCPS measured on the rooftop. (a) Wind speed during the test period. (b) Solar radiation power throughout the test duration. (c) Difference in surface temperature between the OPC and OPCCPS. (d) Measured temperatures of OPC and OPCCPS during the test period.

maximum temperature difference of 6 °C. Notably, the most significant temperature difference between OPCCPS and OPC (Figure 7c) is observed precisely at the peak solar radiation power (Figure 7b), highlighting the remarkable cooling potential of CPS.

Sustainability Benefits. The primary aim of our work is to develop a cool material that contributes to the reduction of CO₂ emissions through two pivotal mechanisms. First, by actively capturing CO₂ during the carbonation process of recycled aggregates, we prevent its release into the atmosphere. Second, the material's high solar reflectance properties help mitigate the UHI effect, subsequently reducing the demand for cooling energy and further lowering the associated CO₂ emissions. The elevated temperature in urban areas strongly affects the energy consumption for cooling. In Santamouris' work,⁴² it was shown that for every degree rise in ambient temperature due to UHI, there is a proportional surge in peak electricity demand, ranging from 0.45–4.6%. In cities where UHI intensification leads to temperature increases of approximately 6 °C, that is corresponding with the temperature reduction observed in our measurements, the associated rise in cooling demand can be substantial. In Rome and Athens, for example, it was calculated that the increase in cooling load can reach as high as 130%.^{43,44} In Beijing, where UHI effects lead to an average temperature increase of 4–6 °C, the additional energy expenditure for air conditioning is estimated to be approximately 815,299 MWh.⁴⁵ Addressing this challenge necessitates innovative approaches, and one promising solution lies in the utilization of cool materials. The solar reflectance (α) is a crucial metric in assessing the

coolness of materials. Studies have demonstrated that an improvement of (α) = 0.2 can yield significant benefits. For instance, in a simulation study encompassing Abu Dhabi, New Delhi, Casablanca, Damascus, and Tokyo, it was estimated that a 0.05 increase in solar reflectance led to a cooling load reduction ranging from 1.34 to 5.7 kW h/m².⁴⁶ Extrapolating this to our concrete with a 0.2 improvement in solar reflectance, we find the potential impact is substantial. The anticipated reduction in cooling load falls between 5.4 and 22.8%, signifying a noteworthy advancement in energy efficiency. Furthermore, our concrete, by incorporation of carbonated aggregates, offers an added dimension of sustainability. This material actively captures CO₂ during the carbonation process, contributing to a decrease in carbon emissions. Studies by Ma et al. have quantified the impact of cement for the construction of 1 km of pavement in China,⁴⁷ revealing that the emissions of 519 thousand tons CO₂ are due to cement raw material production phase. With a carbon capture rate of 18 wt %, this translates to a reduction of 28 000 tons for every kilometer of pavement constructed. Moreover, the use of recycled aggregates further contributes to sustainability efforts, reducing the need for sand and coarse aggregate production, which accounts for approximately 15 million tons of CO₂ emissions for 1 km of pavement.

CONCLUSIONS

This study addressed a critical research gap by investigating the reflective properties of an innovative cool cementitious composite with carbonated recycled aggregates, offering a promising solution for UHI mitigation. PS ash was successfully transformed into CPS, which is primarily composed of calcite, through a carbon capture process. By incorporation of CPS into OPC, a reflective concrete that captured approximately 18 wt % of its weight in carbon dioxide was developed. In terms of solar reflectivity, CPS exhibited exceptional performance with a solar absorption (α) value of 0.11, surpassing commonly used cool paving materials and falling within the recommended range for achieving subambient cooling. Furthermore, the incorporation of CPS as a carbonated aggregate in the carbonated concrete (OPCCPS) led to a substantial improvement in reflectance (+62%) compared to that with OPC. OPCCPS demonstrated a solar absorption (α) value of 0.38 and SRI = 73, showcasing its effectiveness in reducing surface temperatures. Comprehensive rooftop tests further validated the superior performance of the OPCCPS in reducing surface temperatures. With a maximum temperature difference of 6 °C compared to that with OPC, the OPCCPS consistently exhibited lower temperatures, particularly at peak solar radiation power. The successful development of carbonated concrete holds significant implications for sustainable urban development. Through the integration of such elements into urban structural components, there exists the potential to alleviate UHI effects, decrease energy usage and establish urban environments that are both more comfortable and sustainable. Moreover, the remarkably straightforward and easily scalable process of carbonation showcases its adaptability for large-scale implementation. This advancement can play a vital role in shaping future urban planning strategies and promoting the adoption of ecofriendly materials in construction.

AUTHOR INFORMATION

Corresponding Author

Guido Goracci – Centro de Física de Materiales, CSIC-UPV/EHU, San Sebastián E-20018, Spain; orcid.org/0000-0003-2439-3833; Email: guido.goracci@ehu.eus

Authors

Ebtisam Saeed – Centro de Física de Materiales, CSIC-UPV/EHU, San Sebastián E-20018, Spain; Univ. of Bordeaux, CNRS, Bordeaux INP, ICMCB, UMR 5026, Pessac F-33600, France

Mary B. Ogundiran – Centro de Física de Materiales, CSIC-UPV/EHU, San Sebastián E-20018, Spain; Analytical/Environmental Unit, Department of Chemistry, Faculty of Science, University of Ibadan, Ibadan CWV2 + 84, Nigeria

Amaia Iturrospe – Material Physics Center, San Sebastián E-20018, Spain

Arantxa Arbe – Centro de Física de Materiales, CSIC-UPV/EHU, San Sebastián E-20018, Spain

Cyril Aymonier – Univ. of Bordeaux, CNRS, Bordeaux INP, ICMCB, UMR 5026, Pessac F-33600, France; orcid.org/0000-0003-1775-0716

Jorge S. Dolado – Centro de Física de Materiales, CSIC-UPV/EHU, San Sebastián E-20018, Spain; Donostia International Physics Center, San Sebastián 20018, Spain; orcid.org/0000-0003-3686-1438

Complete contact information is available at: <https://pubs.acs.org/10.1021/acssuschemeng.3c05817>

Notes

The authors declare no competing financial interest.

ACKNOWLEDGMENTS

The project has received funding from the European Union's Horizon 2020 research and innovation program under grant agreement no. 964450 (MIRACLE project). Moreover, this work is part of the project TED2021-132074B-C31, funded by MCIN/AEI/10.13039/501100011033 and the EU "Next-GenerationEU"/PRTR. A.I. and A.A. acknowledge the grant PID2021-123438NB-I00 funded by MCIN/AEI/10.13039/501100011033 and by "ERDF A way of making Europe", grant TED2021-130107A-I00 funded by MCIN/AEI/10.13039/501100011033 and Unión Europea "NextGenerationEU/PRTR", as well as the financial support of Eusko Jaurlaritz, code: IT1566-22. MBO acknowledges the financial support from the Women for Africa Foundation (Fundación Mujeres por Africa), Marid, Spain for the research visit and is grateful to the Director, Centro de Física de Materiales, CSIC-UPV/EHU, San Sebastián, Spain for making available the research facilities for the study. We also thank the LTC Green Concrete and the UPV/EHU for the funding of an E. Saeed PhD grant.

REFERENCES

- (1) Wang, C.; Wang, Z.-H.; Kaloush, K. E.; Shacat, J. Cool pavements for urban heat island mitigation: A synthetic review. *Renew. Sustain. Energy Rev.* **2021**, *146*, 111171.
- (2) Santamouris, M. Cooling the cities—a review of reflective and green roof mitigation technologies to fight heat island and improve comfort in urban environments. *Sol. Energy* **2014**, *103*, 682–703.
- (3) Feng, Y.; Wang, J.; Zhou, W.; Li, X.; Yu, X. Evaluating the Cooling Performance of Green Roofs Under Extreme Heat Conditions. *Front. Environ. Sci.* **2022**, *10*, 874614.
- (4) Shafique, M.; Kim, R.; Rafiq, M. Green roof benefits, opportunities and challenges—A review. *Renew. Sustain. Energy Rev.* **2018**, *90*, 757–773.
- (5) Manso, M.; Teotónio, I.; Silva, C. M.; Cruz, C. O. Green roof and green wall benefits and costs: A review of the quantitative evidence. *Renew. Sustain. Energy Rev.* **2021**, *135*, 110111.
- (6) Žuvela-Aloise, M.; Koch, R.; Buchholz, S.; Früh, B. Modelling the potential of green and blue infrastructure to reduce urban heat load in the city of Vienna. *Climatic Change* **2016**, *135*, 425–438.
- (7) Kousis, I.; Pisello, A. Evaluating the performance of cool pavements for urban heat island mitigation under realistic conditions: A systematic review and meta-analysis. *Urban Clim.* **2023**, *49*, 101470.
- (8) Pisello, A. L.; Santamouris, M.; Cotana, F. Active cool roof effect: Impact of cool roofs on cooling system efficiency. *Adv. Build. Energy Res.* **2013**, *7*, 209–221.
- (9) Qin, Y. A review on the development of cool pavements to mitigate urban heat island effect. *Renew. Sustain. Energy Rev.* **2015**, *52*, 445–459.
- (10) Huang, B.; Xiao, Y.; Zhou, H.; Chen, J.; Sun, X. Synthesis and characterization of yellow pigments of Bi₁.7RE₀.3W₀.7Mo₀.3O₆ (RE = Y, Yb, Gd, Lu) with high NIR reflectance. *ACS Sustainable Chem. Eng.* **2018**, *6*, 10735–10741.
- (11) Sharma, R.; Tiwari, S.; Tiwari, S. K. Highly reflective nanostructured titania shell: a sustainable pigment for cool coatings. *ACS Sustainable Chem. Eng.* **2018**, *6*, 2004–2010.
- (12) Xie, N.; Li, H.; Abdelhady, A.; Harvey, J. Laboratorial investigation on optical and thermal properties of cool pavement nano-coatings for urban heat island mitigation. *Build. Environ.* **2019**, *147*, 231–240.
- (13) Zhang, M.; Feng, L.; Zeng, Z.; Yang, Y.; Sun, X. Environmentally Friendly High-Near-Infrared Reflectance Blue Pigment Yn_{0.9-x}Mn_{0.1}O_{3-δ} Based on Li/Zn Doping. *ACS Sustainable Chem. Eng.* **2022**, *10*, 13877–13886.
- (14) Zhang, X.; Li, H.; Xie, N.; Jia, M.; Yang, B.; Li, S. Laboratorial Investigation on Optical and Thermal Properties of Thermochromic Pavement Coatings for Dynamic Thermoregulation and Urban Heat Island Mitigation. *Sustain. Cities Soc.* **2022**, *83*, 103950.
- (15) Karlessi, T.; Santamouris, M.; Apostolakis, K.; Synnefa, A.; Livada, I. Development and testing of thermochromic coatings for buildings and urban structures. *Sol. Energy* **2009**, *83*, 538–551.
- (16) Fabiani, C.; Pisello, A. L.; Bou-Zeid, E.; Yang, J.; Cotana, F. Adaptive measures for mitigating urban heat islands: The potential of thermochromic materials to control roofing energy balance. *Appl. Energy* **2019**, *247*, 155–170.
- (17) Li, N.; Mo, L.; Unluer, C. Emerging CO₂ utilization technologies for construction materials: A review. *J. CO₂ Util.* **2022**, *65*, 102237.
- (18) Liu, B.; Qin, J.; Shi, J.; Jiang, J.; Wu, X.; He, Z. New perspectives on utilization of CO₂ sequestration technologies in cement-based materials. *Constr. Build. Mater.* **2021**, *272*, 121660.
- (19) Chen, T.; Bai, M.; Gao, X. Carbonation curing of cement mortars incorporating carbonated fly ash for performance improvement and CO₂ sequestration. *J. CO₂ Util.* **2021**, *51*, 101633.
- (20) Sharma, D.; Goyal, S. Accelerated carbonation curing of cement mortars containing cement kiln dust: An effective way of CO₂ sequestration and carbon footprint reduction. *J. Clean. Prod.* **2018**, *192*, 844–854.
- (21) Yan, D.; Lu, J.; Sun, Y.; Wang, T.; Meng, T.; Zeng, Q.; Liu, Y. CO₂ pretreatment to aerated concrete with high-volume industry wastes enables a sustainable precast concrete industry. *ACS Sustainable Chem. Eng.* **2021**, *9*, 3363–3375.
- (22) Huang, H.; Guo, R.; Wang, T.; Hu, X.; Garcia, S.; Fang, M.; Luo, Z.; Maroto-Valer, M. M. Carbonation curing for wollastonite-Portland cementitious materials: CO₂ sequestration potential and feasibility assessment. *J. Clean. Prod.* **2019**, *211*, 830–841.
- (23) Monkman, S.; MacDonald, M.; Hooton, R. D.; Sandberg, P. Properties and durability of concrete produced using CO₂ as an accelerating admixture. *Cement Concr. Compos.* **2016**, *74*, 218–224.

- (24) Xian, X.; Zhang, D.; Shao, Y. Flue gas carbonation curing of cement paste and concrete at ambient pressure. *J. Clean. Prod.* **2021**, *313*, 127943.
- (25) Kou, S.-C.; Zhan, B.-j.; Poon, C.-S. Use of a CO₂ curing step to improve the properties of concrete prepared with recycled aggregates. *Cement Concr. Compos.* **2014**, *45*, 22–28.
- (26) Higuchi, T.; Morioka, M.; Yoshioka, I.; Yokozeki, K. Development of a new ecological concrete with CO₂ emissions below zero. *Construct. Build. Mater.* **2014**, *67*, 338–343.
- (27) Pan, X.; Shi, C.; Hu, X.; Ou, Z. Effects of CO₂ surface treatment on strength and permeability of one-day-aged cement mortar. *Constr. Build. Mater.* **2017**, *154*, 1087–1095.
- (28) Zhan, B. J.; Xuan, D. X.; Poon, C. S.; Shi, C. J. Mechanism for rapid hardening of cement pastes under coupled CO₂-water curing regime. *Cement Concr. Compos.* **2019**, *97*, 78–88.
- (29) Regnault, O.; Lagneau, V.; Schneider, H. Experimental measurement of portlandite carbonation kinetics with supercritical CO₂. *Chem. Geol.* **2009**, *265*, 113–121.
- (30) Vance, K.; Falzone, G.; Pignatelli, I.; Bauchy, M.; Balonis, M.; Sant, G. Direct carbonation of Ca (OH) ₂ using liquid and supercritical CO₂: implications for carbon-neutral cementation. *Ind. Eng. Chem. Res.* **2015**, *54*, 8908–8918.
- (31) Saeed, E.; Ogundiram, B. M.; Goracci, G.; Aymonier, C.; Dolado, S. D. Supplementary cementitious materials based on CO₂-Capturing periwinkle shell. *Proceeding 16th International Congress on the Chemistry of Cement*, 2023.
- (32) Kappou, S.; Souliotis, M.; Papaefthimiou, S.; Panaras, G.; Paravantis, J. A.; Michalena, E.; Hills, J. M.; Vouros, A. P.; Ntymenou, A.; Mihalakakou, G. Cool pavements: State of the art and new technologies. *Sustainability* **2022**, *14*, 5159.
- (33) Kyriakodis, G.; Santamouris, M. Using reflective pavements to mitigate urban heat island in warm climates-Results from a large scale urban mitigation project. *Urban Clim.* **2018**, *24*, 326–339.
- (34) Andersen, F. A.; Brečević, L.; Beuter, G.; Dell'Amico, D. B.; Calderazzo, F.; Bjerrum, N. J.; Underhill, A. E. Infrared spectra of amorphous and crystalline calcium carbonate. *Acta Chem. Scand.* **1991**, *45*, 1018–1024.
- (35) Villain, G.; Thiery, M.; Platret, G. Measurement methods of carbonation profiles in concrete: Thermogravimetry, chemical analysis and gammadensimetry. *Cement Concr. Res.* **2007**, *37*, 1182–1192.
- (36) Taylor, H. F.; et al. *Cement Chemistry*; Thomas Telford London, 1997; Vol. 2.
- (37) Ye, G.; Liu, X.; De Schutter, G.; Poppe, A.-M.; Taerwe, L. Influence of limestone powder used as filler in SCC on hydration and microstructure of cement pastes. *Cement Concr. Compos.* **2007**, *29*, 94–102.
- (38) Santamouris, M.; Synnefa, A.; Karlessi, T. Using advanced cool materials in the urban built environment to mitigate heat islands and improve thermal comfort conditions. *Sol. Energy* **2011**, *85*, 3085–3102.
- (39) Mandal, J.; Fu, Y.; Overvig, A. C.; Jia, M.; Sun, K.; Shi, N. N.; Zhou, H.; Xiao, X.; Yu, N.; Yang, Y. Hierarchically porous polymer coatings for highly efficient passive daytime radiative cooling. *Science* **2018**, *362*, 315–319.
- (40) Dolado, J. S.; Goracci, G.; Arrese-Igor, S.; Ayuela, A.; Torres, A.; Liberal, I.; Beruete, M.; Gaitero, J. J.; Cagnoni, M.; Cappelluti, F. Radiative Cooling Properties of Portlandite and Tobermorite: Two Cementitious Minerals of Great Relevance in Concrete Science and Technology. *ACS Appl. Opt. Mater.* **2023**.
- (41) Liu, D.; Kaja, A.; Zepper, J.; Fan, D.; Zhang, D.; Brouwers, H.; Yu, Q. Scalable cooling cementitious Composites: Synergy between Reflective, Radiative, and Evaporative cooling. *Energy Build.* **2023**, *285*, 112909.
- (42) Santamouris, M. On the energy impact of urban heat island and global warming on buildings. *Energy Build.* **2014**, *82*, 100–113.
- (43) Fanchiotti, A.; Carnielo, E.; Zinzi, M. Impact of cool materials on urban heat islands and on buildings comfort and energy consumption. *Proceedings of the American Solar Energy Society National Conference*, 2012.
- (44) Santamouris, M.; Papanikolaou, N.; Livada, I.; Koronakis, I.; Georgakis, C.; Argiriou, A.; Assimakopoulos, D. On the impact of urban climate on the energy consumption of buildings. *Sol. Energy* **2001**, *70*, 201–216.
- (45) Li, C.; Zhou, J.; Cao, Y.; Zhong, J.; Liu, Y.; Kang, C.; Tan, Y. Interaction between urban microclimate and electric air-conditioning energy consumption during high temperature season. *Appl. Energy* **2014**, *117*, 149–156.
- (46) Synnefa, A.; Santamouris, M.; Akbari, H. Estimating the effect of using cool coatings on energy loads and thermal comfort in residential buildings in various climatic conditions. *Energy Build.* **2007**, *39*, 1167–1174.
- (47) Ma, F.; Sha, A.; Yang, P.; Huang, Y. The greenhouse gas emission from Portland cement concrete pavement construction in China. *Int. J. Environ. Res. Publ. Health* **2016**, *13*, 632.